
Graph Representation Learning Network via Adaptive Sampling

Anderson de Andrade
Wattpad
Toronto, Ontario, Canada
anderson@wattpad.com

Chen Liu
Wattpad
Toronto, Ontario, Canada
cecilia@wattpad.com

Abstract

Graph Attention Network (GAT) and GraphSAGE are neural network architectures that operate on graph-structured data and have been widely studied for link prediction and node classification. One challenge raised by GraphSAGE is how to smartly combine neighbour features based on graph structure. GAT handles this problem through attention, however the challenge with GAT is its scalability over large and dense graphs. In this work, we proposed a new architecture to address these issues that is more efficient and is capable of incorporating different edge type information. It generates node representations by attending to neighbours sampled from weighted multi-step transition probabilities. We conduct experiments on both transductive and inductive settings. Experiments achieved comparable or better results on several graph benchmarks, including the Cora, Citeseer, Pubmed, PPI, Twitter, and YouTube datasets.

1 Introduction

Graphs are a versatile and succinct way to describe entities through their relationships. The information contained in many knowledge graphs (KG) has been used in several machine learning tasks in natural language understanding [20], computer vision [16], and recommendation systems [29]. The same information can also be used to expand the graph itself via node classification [11], clustering [19], or link prediction tasks [14], in both transductive and inductive settings [15].

Recent graph models have focused on learning dense representations that capture the properties of a node and its neighbours. One class of methods generates spectral representation for nodes [3, 7]. The rigidity of this approach may reduce the adaptability of a model to graphs with structural differences.

Model architectures that reduce the neighbourhood of a node have used pooling [13], convolutions [9], recurrent neural networks (RNN) [17], and attention [28]. These approaches often require many computationally-expensive message-passing iterations to generate representations for the neighbours of a target node. Sparse Graph Attention Networks (SGAT) [30] was proposed to address this inefficiency by producing an edge-sparsified graph. However, it may neglect the importance of local structure when graphs are large or have multiple edge types. Other methods have used objective functions to predict whether a node belongs to a neighbourhood [19, 14], for example by using noise-contrastive estimation [12]. However, incorporating additional training objectives into a downstream task can be difficult to optimize, leading to a multi-step training process.

In this work, we present a graph network architecture (GATAS) that can be easily integrated into any model and supports general graph types, such as: cyclic, directed, and heterogeneous graphs. The method uses a self-attention mechanism over a multi-step neighbourhood sample, where the transition probability of a neighbour at a given step is parameterized.

We evaluate the proposed method in node classification tasks using the Cora, Citeseer and Pubmed citation networks in a transductive setting, and on a protein to protein interaction (PPI) dataset in an inductive setting. We also evaluate the method on a link prediction task using a Twitter and YouTube dataset. Results show that the proposed graph network can achieve better or comparable performance to state-of-the-art architectures.

2 Related Work

The proposed architecture is related to GraphSAGE [13], which also reduces neighbour representations from fixed-size samples. Instead of aggregating uniformly-sampled 1-hop neighbours at each depth, we propose a single reduction of multi-step neighbours sampled from parameterized transition probabilities. Such parameterization is akin to the Graph Attention Model [1], where trainable depth coefficients scale the transition probabilities from each step. Thus, the model can choose the depth of the neighbourhood samples. We further extend this approach to transition probabilities that account for paths with heterogeneous edge types.

We use an attention mechanism similar to the one in Graph Attention Networks (GAT) [28]. While GAT reduces immediate neighbours iteratively to explore the graph structure in a breadth-first approach that processes all nodes and edges at each step, our method uses multi-step neighbourhood samples to explore the graph structure. Our method also allows each neighbour to have a different representation for the target node, rather than using a single representation as in GAT.

MoNet [18] generalizes many graph convolutional networks (GCN) as attention mechanisms. More recently, the edge-enhanced graph neural network framework (EGNN) [10] consolidates GCNs and GAT. In MoNet, the attention coefficient function only uses the structure of the nodes. In addition, our model employs node representations to generate attention weights.

Other approaches use recurrent neural networks [22, 17] to reduce path information between neighbours and generate node representations. The propagation algorithm in Gated Graph Neural Networks (GG-NNs) [17] reduces neighbours one step at a time, in a breadth-first fashion. In contrast, we use a depth-first approach where a reduction operation is applied across edges of a path.

3 Model

3.1 Preliminaries

An initial graph is defined as $\mathcal{G} = (\mathcal{V}, \mathcal{R}, \mathcal{Z})$, where $\mathcal{V} = \{v_1, \dots, v_{|\mathcal{V}|}\}$ is a set of nodes or vertices, $\mathcal{R} = \{r_1, \dots, r_{|\mathcal{R}|}\}$ is a set of edge types or relations, and $\mathcal{Z} = \{(v_i, r_k, v_j) \mid v_i, v_j \in \mathcal{V}; r_k \in \mathcal{R}\}$ is a set of triplets. Directed graphs are represented by having one edge type for each direction so that $(v_i, r^+, v_j) \in \mathcal{Z} \iff (v_j, r^-, v_i) \in \mathcal{Z}$. To be able to incorporate information about the target node, the graph \mathcal{G} is augmented with self-loops using a new edge type r_\emptyset . Thus, a new set of edge types $\tilde{\mathcal{R}} = \{r_\emptyset\} \cup \mathcal{R}$ is created such that $\tilde{r}_1 = r_\emptyset$, and a new set of triplets $\tilde{\mathcal{Z}} = \{(v_i, r_\emptyset, v_i) \mid v_i \in \mathcal{V}\} \cup \{(v_i, r_{k+1}, v_j) \mid (v_i, r_k, v_j) \in \mathcal{Z}\}$ conforms a new graph $\tilde{\mathcal{G}} = (\mathcal{V}, \tilde{\mathcal{R}}, \tilde{\mathcal{Z}})$.

An edge type path between nodes v_i and v_j is defined as $E^{(i,j)} = (a_t \mid \tilde{r}_{a_t} \in \tilde{\mathcal{R}})_{t=1}^{\leq C}$, where $C \geq 1$ is the maximum number of steps considered. The number of all possible edge type paths is given by $M = \sum_{t=1}^C |\tilde{\mathcal{R}}|^t$. The set of all possible edge type paths is defined as $\mathcal{E} = \{E_1, \dots, E_M\}$. The edge type sequences in the set are level-ordered so that $\forall m \in \{1, \dots, M-1\}, |E_m| \leq |E_{m+1}|$, and so that $\forall m, n \in \{(m, n) : |E_m| = |E_n|, m < n\}, \forall i \in \{1, \dots, |E_{m,i}|\}, E_{m,i} \leq E_{n,i}$. As an example, if $\tilde{\mathcal{R}} = \{A, B\}$ and $C = 2$, then \mathcal{E} corresponds to: $\{(A), (B), (A, A), (A, B), (B, A), (B, B)\}$. The subset of relation paths connecting nodes $v_i \rightarrow v_j$ is defined as $\mathcal{E}^{(i,j)} = \{E_m^{(i,j)} \mid E_m \in \mathcal{E}\}$, where $\mathcal{E}^{(i,j)} = \{E_1\} \Rightarrow i = j$ represents the extraneous self-loops.

3.2 Neighbour Representations

Graph relations in $\tilde{\mathcal{R}}$ are represented by trainable vectors $\mathbf{e} = \{\vec{e}_1, \dots, \vec{e}_{|\tilde{\mathcal{R}}|}\}, \vec{e} \in \mathbb{R}^D$. To reflect the position in a path, the edge representations can be infused with information that reflects its position in a path. Following [27], we assign a sinusoid of a different wavelength to each dimension, each

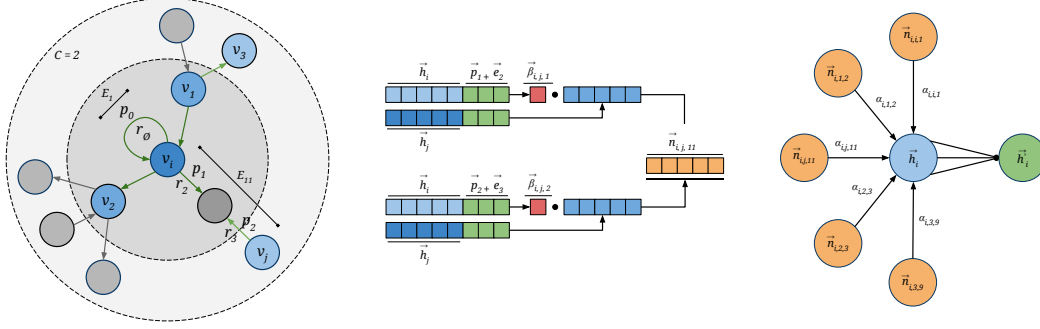


Figure 1: **Left:** An illustration of the multi-step sampling technique with relevant notation presented in this work. Blue nodes represent sampled nodes. The edge type path E_{11} is detailed. **Center:** The attention mechanism for $E_{11} \in \mathcal{E}^{(i,j)}$ that generates the neighbour representation $\vec{n}_{i,j,11}$. **Right:** The attention mechanism by target node v_i . Neighbour representations are aggregated according to the attention weights.

position being a different point:

$$\vec{p}_{t,2i} = \sin(t/10000^{2i/D}), \vec{p}_{t,2i+1} = \cos(t/10000^{2i/D})$$

where $t : 0 \leq t \leq C$ is the position in an edge type path and $i : 0 \leq i < D/2$ is the index of the dimension.

We represent nodes as a set of vectors $\vec{\mathbf{h}} = \{\vec{h}_1, \dots, \vec{h}_{|V|}\}, \vec{h}_i \in \mathbb{R}^{F+R}$. Each vector is defined by $\vec{h}_i = [\vec{l}_i \| \vec{b}_i]$, where $\vec{l}_i \in \mathbb{R}^R$ are trainable embedding representations and $\vec{b}_i \in \mathbb{R}^F; \vec{b}_i \in \vec{\mathbf{b}} = \{\vec{b}_1, \dots, \vec{b}_{|V|}\}$ represents the features of the node. The learnable embedding representations can capture information to support a neighbourhood sample.

Given an edge type path $E_m \in \mathcal{E}^{(i,j)} | i \neq j$, we generate a neighbour representation $\vec{n}_{i,j,m}$ using attention over transformed neighbour representations for each edge type in E_m :

$$\vec{n}_{i,j,m} = \sum_{t=1}^{|E_m|} \beta_{i,m,t} z([\vec{h}_j \| \vec{e}_{E_m,t} + \vec{p}_t]), \beta_{i,m,t} = \frac{\exp(f([\vec{h}_i \| \vec{e}_{E_m,t} + \vec{p}_t]))}{\sum_{x=1}^{|E_m|} \exp(f([\vec{h}_i \| \vec{e}_{E_m,x} + \vec{p}_x]))} \quad (1)$$

where $z : \mathbb{R}^{F+R+D} \rightarrow \mathbb{R}^{F'}$ and $f : \mathbb{R}^{F+R+D} \rightarrow \mathbb{R}$ are two different learnable transformations. The transformation given by z allows neighbour representations to be different according to the edge type in the path. For the self-loop edge type path E_1 , we set $\vec{n}_{i,j,1} = z([\vec{h}_i \| \vec{e}_1 + \vec{p}_0])$.

3.3 Transition Tensors

We define transition probability distributions for neighbours and their possible edge type paths within $[1, C]$ steps. When there are multiple edges types connecting two nodes, their transition probabilities split. Thus, when computing transition probabilities for random walks starting at v_i , it is necessary to track the probability of an edge type path $E_m \in \mathcal{E}^{(i,j)}$ for each destination vertex v_j , effectively computing $P(v_j, \mathcal{E}|v_i)$. Also, when performing random walks from a starting node v_i , we break cycles by disallowing transitions to nodes already visited in previous steps. This reduces $\mathcal{E}^{(i,j)}$ to the set of shortest $v_i \rightarrow v_j$ edge type paths possible.

Let $\mathbf{A} \in \{0, 1\}^{|\mathcal{V}| \times |\mathcal{V}| \times M}$ be a sparse adjacency tensor for $\tilde{\mathcal{G}}$, where:

$$A_{i,j,m} = \begin{cases} 1, & \text{if } (v_i, \tilde{r}_m, v_j) \in \tilde{\mathcal{Z}} \wedge 1 < m \leq |\tilde{\mathcal{R}}| \\ 0, & \text{otherwise} \end{cases}$$

An initial transition tensor $\mathbf{T}^{(1)} \in \mathbb{R}^{|\mathcal{V}| \times |\mathcal{V}| \times M}$ can be computed by normalizing the $\mathbf{A}_{v,*,*}$ matrices to sum to one, when applying the function $\Psi : \mathbb{R}^{|\mathcal{V}| \times |\mathcal{V}| \times M} \rightarrow \mathbb{R}^{|\mathcal{V}| \times |\mathcal{V}| \times M}$:

$$\Psi(\mathbf{Z})_{i,j,m} = \frac{Z_{i,j,m}}{\sum_{x=1}^{|\mathcal{V}|} \sum_{y=1}^M Z_{i,x,y}}$$

Using the order in \mathcal{E} to obtain the probabilities for specific edge type paths, the unnormalized sparse transition tensor $\tilde{\mathbf{T}}^{(t)}$ for steps $1 < t \leq C$ can be computed as follows:

$$\tilde{T}_{i,j,m}^{(t)} = \begin{cases} \sum_{x=1}^{|\mathcal{V}|} T_{i,x,\phi(m)}^{(1)} T_{i,x,\delta(m)}^{(t-1)}, & \text{if } \sum_{y=1}^M T_{i,j,y}^{(l)} = 0, \forall l \in \{1, \dots, t-1\} \\ 0, & \text{otherwise} \end{cases} \quad (2)$$

where $\phi(m) = (m-1) \bmod |\tilde{\mathcal{R}}| + 1$ specifies the edge type \tilde{r}_k for the last step in path E_m , and $\delta(m) = \lfloor (m-1)/|\tilde{\mathcal{R}}| \rfloor$ is the edge type path E_n without the last step in E_m . As an example, if E_m is the sequence of relation indices that corresponds to $\{A, B, C\}$, then $E_{\delta(m)}$ corresponds to $\{A, B\}$, and $E_{\phi(m)}$ corresponds to C .

The conditional function in Equation 2 sets the transition probability to zero if the node v_j can be reached from v_i in a previous step t . This procedure effectively breaks cycles and allows only the most relevant and shortest edge type paths to be sampled. A normalized transition tensor is obtained by $\mathbf{T}^{(t)} = \Psi(\tilde{\mathbf{T}}^{(t)})$.

3.4 Neighbourhood Sampling

When considering a neighbourhood $N_i = \{(j, m) \mid v_j \in \mathcal{V}, E_m \in \mathcal{E}^{(i,j)}\}$, it can be relevant to attend to nodes beyond the first degree neighbourhood. However, as the number of hops between nodes increases, their relationship weakens. It can also be prohibitive to attend to all nodes within C hops, as the neighbourhood size $|N_i|$ grows proportionally with $C \times \mathbb{E}_{v \in |\mathcal{V}|}[\text{degree}(v)]^C$.

To overcome these complications, we create a fixed-size neighbourhood sample from an adjustable transition tensor $\mathbf{P} \in \mathbb{R}^{|\mathcal{V}| \times |\mathcal{V}| \times M}$. Similar to the work in [1], we obtain neighbour probabilities by a linear combination of random walk transition tensors for each step k , with learnable coefficients \mathbf{q} :

$$\mathbf{P} = \sum_{t=0}^C q_t \mathbf{T}^{(t)}$$

where $(q_0, \dots, q_C) = \text{softmax}(\tilde{q}_0, \dots, \tilde{q}_C)$ and $\tilde{\mathbf{q}} \in \mathbb{R}^{C+1}$ is a vector of unbounded parameters. $\mathbf{T}^{(0)}$ corresponds to a transition tensor for the added self-loops:

$$T_{i,j,m}^{(0)} = \begin{cases} 1, & \text{if } (v_i, r_\emptyset, v_j) \in \tilde{\mathcal{Z}} \wedge m = 1 \\ 0, & \text{otherwise} \end{cases}$$

Depending on the task and graph, the model can control the scope of the neighbourhood by adjusting these coefficients through backpropagation.

To generate a neighbourhood N_i for $v_i \in \mathcal{V}$ we sample without replacement from \mathbf{P} so that $N_i = \{(j, m) \mid (j, m) \sim \mathbf{P}_{i,*,*}\}^S$, where S is the maximum size for a neighbourhood sample.

3.5 Node Representations

Given a neighbourhood N_i for node $v_i \in V$ and a transition tensor \mathbf{P} , we apply an attention mechanism with attention coefficients given by:

$$\alpha_{i,j,m}^{(k)} = \frac{\exp[g^{(k)}([\vec{h}_i \parallel \vec{n}_{i,j,m}])] + \ln(P_{i,j,m})}{\sum_{(x,y) \in N_i} \exp[g^{(k)}([\vec{h}_i \parallel \vec{n}_{i,x,y}])] + \ln(P_{i,x,y})} \quad (3)$$

where $g^{(k)} : \mathbb{R}^{F'} \rightarrow \mathbb{R}$ is a learnable transformation. The logits produced by $g^{(k)}$ are scaled by the transition probabilities, exerting the importance of the neighbour, and allowing the coefficients \mathbf{q} to be trained. We concatenate multi-head attention layers to create a new node representation \vec{h}'_i :

$$\vec{h}'_i = \left\| \right\|_{k=1}^K \sigma \left(\sum_{(j,m) \in N_i} \alpha_{i,j,m}^{(k)} d^{(k)}(\vec{n}_{i,j,m}) \right) \quad (4)$$

where $d^{(k)} : \mathbb{R}^{F'} \rightarrow \mathbb{R}^{F''}$ is another learnable transformation, and $\sigma : \mathbb{R} \rightarrow \mathbb{R}$ is a non-linear activation function, such as the ELU [5] function. The transformation allows relevant information for the node to be selected.

3.6 Algorithmic Complexity

The complexity of generating node representations with the proposed algorithm (GATAS) is governed by $\mathcal{O}(C \times S \times B \times F_{max})$, where B is the batch size and $F_{max} = \max(F + R + D, F', F'')$. GraphSAGE [13] has a similar complexity of $\mathcal{O}(S^C \times B \times F)$. GAT [28] on the other hand, has a complexity that is independent of the batch size but processes all nodes and edges. It is given by $\mathcal{O}(C \times (|\mathcal{V}| \times F + |\tilde{\mathcal{Z}}|))$, where C is the number of layers that controls depth. For downstream tasks where only a small subset of nodes are actually used, the overhead complexity of GAT can be overwhelming. Generalizing, our model is more efficient when $|\mathcal{V}| + |\tilde{\mathcal{Z}}| > B \times S$.

4 Evaluation

We evaluate the performance of GATAS using node classification tasks in transductive and inductive settings. To evaluate the performance of the proposed attention mechanism over heterogeneous multi-step neighbours, we rely on a multi-class link prediction task.

For the transductive learning experiments we compare against GAT [28] and some of the approaches specified in [15], including a CNN approach that uses Chebyshev approximations of the graph eigendecomposition [7], the Graph Convolutional Network (GCN) [15], MoNet [18], and the Sparse Graph Attention Network (SGAT) [30]. We also benchmark against a multi-layer perceptron (MLP) that classifies nodes only using its features without any graph structure.

For the inductive experiments we compare once again against GAT [28] and SGAT [30]. We also compare against GraphSAGE [13], a method that aggregates node representations from fixed-size neighbourhood samples, using different methods such as LSTMs and max-pooling.

GATAS is capable of utilizing edge information, which we consider to be an important advantage. Hence we also conducted link prediction experiments on multiplex heterogeneous network datasets against some of the state-of-the-art models, namely GATNE[4], MNE[31], and MVE[21]. GATNE creates multiple representations for a node under different edge type graphs, aggregates these individual views using reduction operations similar to GraphSAGE, and combines these node representations using attention.

4.1 Datasets

For the transductive node classification tasks we use three standard citation network datasets: Cora, Citeseer, and Pubmed [23]. In these datasets, each node corresponds to a publication and undirected edges represent citations. Training sets contain 20 nodes per class. The validation and test sets have 500 and 1000 unseen nodes respectively.

For the inductive node classification experiments, we use the protein interaction dataset (PPI) in [13]. The dataset has multiple graphs, where each node is a protein, and undirected edges represent an interaction between them. Each graph corresponds to a different type of interaction between proteins. 20 graphs are used for training, 2 for validation and another 2 for testing.

For the link prediction task, we use the heterogeneous Higgs Twitter Dataset¹ [6]. It is made up of four directional relationships between more than 450,000 Twitter users. We also use a multiplex bidirectional network dataset that consists of five types of interactions between 15,088 YouTube users [25, 26]. Using the dataset splits provided by the authors of GATNE², we work with subsets of 10,000 and 2,000 nodes for Twitter and YouTube respectively, reserving 5% and 10% of the edges for validation and testing. Each split is augmented with the same amount of non-existing edges, that are used as negative samples.

Detailed statistics for these datasets are summarized in Table 4 in Supplementary Materials.

4.2 Experiment Setup

Node features are normalized using layer normalization [2]. These features are then passed through a single dense layer to obtain the input features $\vec{\mathbf{b}}$. The Twitter dataset does not provide node features

¹<http://snap.stanford.edu/data/higgs-twitter.html>

²<http://github.com/thudm/gatne>

Table 1: Node Classification Results

Model	Transductive (Accuracy %)			Inductive (Micro-F1)
	Cora	Citeseer	Pubmed	PPI
MLP	55.1%	46.5%	71.4%	0.422
Chebyshev [7]	81.2%	69.8%	74.4%	—
GCN [15]	81.5%	70.3%	79.0%	—
MoNet [18]	81.7% \pm 0.5%	—	78.8% \pm 0.3%	—
GraphSAGE [13]	—	—	—	0.768
GAT [28]	83.0% \pm 0.7%	72.5% \pm 0.7%	79.0% \pm 0.3%	0.973 \pm 0.002
SGAT* [30]	84.2%	68.2%	77.6%	0.966
GATAS ₁₀	80.2% \pm 1.1%	69.4% \pm 1.3%	76.1% \pm 0.8%	0.818 \pm 0.015
GATAS ₁₀₀	82.3% \pm 0.9%	69.6% \pm 1.1%	78.4% \pm 0.6%	0.981 \pm 0.002
GATAS ₅₀₀	82.1% \pm 0.8%	69.7% \pm 1.4%	78.7% \pm 0.6%	0.985 \pm 0.001

* We selected the best results reported by SGAT.

so $\vec{\mathbf{h}} = \vec{\mathbf{I}}$. The inductive node classification task does not use learnable node embeddings so $\vec{\mathbf{h}} = \vec{\mathbf{b}}$. We define $f(\cdot)$ as a linear transformation, $g^{(k)}(\cdot)$ as a two-layer neural network with a non-linear hidden layer and a linear output layer, and $z(\cdot)$ and $d^{(k)}(\cdot)$ as one-layer non-linear neural networks. Non-linear layers use ELU [5] activation functions.

For all models we set $F, F', F'' = 50$. We experimented with learnable node embeddings and edge type embedding sizes of 10 and 50 for the transductive node classification and link prediction tasks respectively. We use an edge type embedding size of 5 for the inductive tasks. The transductive tasks have 8 attention heads, while the other tasks have 10 heads.

For the transductive node classification tasks, the output layer is directly connected to the concatenated attention heads. For the inductive task, the concatenated attention heads are passed through 2 non-linear layers before going through the output layer. In the link prediction task, the concatenated attention heads are passed through a non-linear layer and a pair of corresponding node representations are concatenated before they pass through 2 non-linear layers and an output layer. All these hidden layers have a size of 256.

The optimization objective is the multi-class or multi-label cross-entropy, depending on the task. It is minimized by the Nadam SGD optimizer [8]. The validation set is used for early stopping and hyper-parameter tuning. Since the training sets for the transductive node classification tasks are very small, it is crucial to add noise to the model inputs to prevent overfitting. We mask out input features with 0.9 probability, and apply Dropout [24] with 0.5 probability to the attention coefficients and resulting representations. We also add L_2 regularization with $\lambda = 0.05$.

In the node classification and link prediction tasks, neighbourhood candidates can be at most 3 and 2 steps C away from the target node respectively. The unnormalized transition coefficients are initialized with a non-linear decay given by $\tilde{q}_t = -t/\ln(C + 1)$. To accommodate for an inductive setting, edges across graphs in the protein interaction dataset are treated as the same type and use the same edge type representations. In the link prediction task we reuse the node representations during test time and rely on the neighbours given by the edges in the training set.

The experiment parameters are summarized in Table 5 in Supplementary Materials. In the transductive node classification experiments, the architecture hyper-parameters were optimized on the Cora dataset and are reused for Citeseer and Pubmed. A single experiment can be run on a V100 GPU under 12 hours. Implementation code is available on GitHub³.

4.3 Results

Table 1 summarizes our results on the node classification tasks. For the transductive tasks, we report the mean classification accuracy and standard deviation over 100 runs. For the inductive task, we

³<http://github.com/wattpad/gatas>

Table 2: Link Prediction Results

Dataset	MVE[21]		MNE[31]		GATNE-T[4]		GATAS ₁₀₀	
	ROC-AUC	F1	ROC-AUC	F1	ROC-AUC	F1	ROC-AUC	F1
Twitter*	72.62	67.40	91.37	84.32	92.30	84.96	95.44	87.13
YouTube*	70.39	65.10	82.30	75.03	84.61	76.83	96.63	83.59

* Results reported for GATNE, MNE and MVE are from the original GATNE paper [4].

report the mean micro-F1 score and standard deviation over 10 runs. We compare against the metrics already reported in [28, 15], and use the same dataset splits provided. For GraphSAGE, we report the better results obtained in [28].

Using the settings described in the previous section, we provide variations of our method using different neighbourhood sample sizes: 10, 100, and 500. We notice that the model can achieve comparable performance, and that we have achieved a new state-of-the-art performance on the PPI dataset in an inductive setting, by a 1.2% margin.

Performance increases with the neighbourhood sample size, as it expands the graph structure covered. However, we do not see substantial improvements for a sample size of 500. Given the average number of neighbours per node for each dataset, as shown in Table 1, we can see that an increased neighbourhood sample size of 500 might not add additional neighbours to the models in the transductive experiments. However, for the PPI dataset, 500 is still significantly below an estimated average neighbourhood size of 28.3^C , where $C = 3$ is the number of steps considered.

We note that in the PPI dataset, a small neighbourhood sample size of 10 impacts performance considerably more than in the transductive setting. This could be because there is no support from the learnable node representations. As the amount of information provided by neighbours decreases, the model might become more dependent on these parameters. The proposed neighbourhood sampling technique trades in a small amount of accuracy to gain efficiency. As a result, the model can easily be used with large datasets and downstream tasks.

Table 2 summarizes our results on the link prediction task. We report the macro area under the ROC curve and the macro F1 score for a single run. When comparing against GATNE, we use the transductive version of the model since we do not precompute raw features for the nodes and rely on the learned representations during test time.

The results suggest the produced node representations are able to capture path attributes as part of the neighbourhood information. GATAS outperforms GATNE-T, with a lift of 3.14% and 12.02% in ROC-AUC, as well as 3.17% and 6.76% in the F1 score, on the Twitter and YouTube datasets respectively. The results achieved new state-of-the-art performances, to the best of our knowledge.

4.4 Ablation Study

The proposed architecture has three independent components that have not been considered in previous work: (1) the neighbour sampling technique using transition probabilities with learnable step coefficients that affect the attention weights; (2) the learnable node representations $\tilde{\mathbf{I}}$ that augment node features with neighbourhood information; and (3) the attention network that allows neighbour representations to adapt to the target node given itself and the path information.

In this section we measure the impact of each component on the Cora and Pubmed datasets for the transductive setting and the PPI dataset for the inductive setting. We consider five model variations that test the importance of each component. All variations of the inductive models do not use learnable node representations because of the nature of its setting. We would like to test the importance of edge type information but the link prediction datasets do not provide node features that would allow us to run all variations. We define the following variations:

- **Base** only samples immediate neighbours with uniform probability and the transition probabilities are not part of the attention weights. The model does not adapt neighbour represen-

Table 3: Ablation Study Results

Model	Transductive (Accuracy %)		Inductive (Micro-F1)
	Cora	Pubmed	PPI
Base	79.3% \pm 0.7%	76.2% \pm 0.7%	0.974 \pm 0.001
GATAS w/o trans	76.7% \pm 0.8%	77.8% \pm 0.5%	0.982 \pm 0.001
GATAS w/o embed	82.2% \pm 0.7%	78.3% \pm 0.8%	—
GATAS w/o paths	82.3% \pm 0.7%	78.4% \pm 0.7%	0.983 \pm 0.001
GATAS	82.3% \pm 0.9%	78.4% \pm 0.6%	0.985 \pm 0.001

tations and nodes do not include learnable representations. Neighbour representations are reduced using the attention mechanism described in Section 3.5.

- **GATAS w/o trans** is the proposed solution but all nodes within $C = 3$ steps can be sampled with uniform probability and the transition probabilities are not part of the attention weights.
- **GATAS w/o embed** is the proposed solution but only node features are used such that $\vec{h} = \vec{b}$ and \vec{I} is not used. This variation is not available for the inductive task because of its nature.
- **GATAS w/o paths** corresponds to the proposed solution but neighbour representations are not transformed according to the target node and path information.
- **GATAS** is the proposed solution.

We ran experiments using the same settings described in Section 4.2. In all the transductive variations, we use a sample size $S = 100$, since a larger value might attenuate the impact of using learnable representations, interfering with the results of the *GATAS w/o embed* variation. For the variations in the inductive task we use a sample size of $S = 500$.

Table 3 shows our results. The largest jump in performance corresponds to the use of the neighbourhood sampling technique and incorporation of the transition probabilities. The use of learnable embeddings as part of node representations does not seem to cause a big impact on performance but this could be a consequence of a large neighbourhood size S , which might reduce the need to utilize these parameters. Finally, the use of adaptable neighbour representations does not seem to affect performance for these tasks. We hypothesize that the nature of the tasks might not require such neighbour transformations but note that edge direction and different edge types are not present in these datasets.

5 Conclusion

In this paper, we proposed a new neural network architecture for graphs. The algorithm represents nodes by reducing their neighbour representations with attention. Multi-step neighbour representations incorporate different path properties. Neighbours are sampled using learnable depth coefficients.

Our model achieves comparable results across different tasks and various baselines, on the benchmark datasets: Cora, Citeseer, Pubmed, PPI, Twitter and YouTube. We successfully retained performance while increasing efficiency on large graphs, achieving state-of-the-art performance on multiple datasets from different tasks. We conducted an ablation study in transductive and inductive settings. The experiments show that sampling neighbourhoods according to weighted transition probabilities achieves the largest performance gain, especially in the inductive setting.

References

- [1] Sami Abu-El-Haija, Bryan Perozzi, Rami Al-Rfou, and Alexander A Alemi. Watch your step: Learning node embeddings via graph attention. In *Advances in Neural Information Processing Systems*, pages 9180–9190, 2018.
- [2] Jimmy Lei Ba, Jamie Ryan Kiros, and Geoffrey E Hinton. Layer normalization. *arXiv preprint arXiv:1607.06450*, 2016.

- [3] Joan Bruna, Wojciech Zaremba, Arthur Szlam, and Yann LeCun. Spectral networks and locally connected networks on graphs. *arXiv preprint arXiv:1312.6203*, 2013.
- [4] Yukuo Cen, Xu Zou, Jianwei Zhang, Hongxia Yang, Jingren Zhou, and Jie Tang. Representation learning for attributed multiplex heterogeneous network. In *Proceedings of the 25th ACM SIGKDD International Conference on Knowledge Discovery & Data Mining*, pages 1358–1368, 2019.
- [5] Djork-Arné Clevert, Thomas Unterthiner, and Sepp Hochreiter. Fast and accurate deep network learning by exponential linear units (elus). *arXiv preprint arXiv:1511.07289*, 2015.
- [6] Manlio De Domenico, Antonio Lima, Paul Mougél, and Mirco Musolesi. The anatomy of a scientific rumor. *Scientific reports*, 3:2980, 2013.
- [7] Michaël Defferrard, Xavier Bresson, and Pierre Vandergheynst. Convolutional neural networks on graphs with fast localized spectral filtering. In *Advances in neural information processing systems*, pages 3844–3852, 2016.
- [8] Timothy Dozat. Incorporating nesterov momentum into adam. 2016.
- [9] David K Duvenaud, Dougal Maclaurin, Jorge Iparraguirre, Rafael Bombarell, Timothy Hirzel, Alán Aspuru-Guzik, and Ryan P Adams. Convolutional networks on graphs for learning molecular fingerprints. In *Advances in neural information processing systems*, pages 2224–2232, 2015.
- [10] Liyu Gong and Qiang Cheng. Exploiting edge features for graph neural networks. In *Proceedings of the IEEE Conference on Computer Vision and Pattern Recognition*, pages 9211–9219, 2019.
- [11] Aditya Grover and Jure Leskovec. node2vec: Scalable feature learning for networks. In *Proceedings of the 22nd ACM SIGKDD international conference on Knowledge discovery and data mining*, pages 855–864. ACM, 2016.
- [12] Michael U Gutmann and Aapo Hyvärinen. Noise-contrastive estimation of unnormalized statistical models, with applications to natural image statistics. *Journal of Machine Learning Research*, 13(Feb):307–361, 2012.
- [13] Will Hamilton, Zhitao Ying, and Jure Leskovec. Inductive representation learning on large graphs. In *Advances in Neural Information Processing Systems*, pages 1024–1034, 2017.
- [14] Seyed Mehran Kazemi and David Poole. Simple embedding for link prediction in knowledge graphs. In *Advances in Neural Information Processing Systems*, pages 4284–4295, 2018.
- [15] Thomas N Kipf and Max Welling. Semi-supervised classification with graph convolutional networks. *arXiv preprint arXiv:1609.02907*, 2016.
- [16] Ruiyu Li, Makarand Tapaswi, Renjie Liao, Jiaya Jia, Raquel Urtasun, and Sanja Fidler. Situation recognition with graph neural networks. In *Proceedings of the IEEE International Conference on Computer Vision*, pages 4173–4182, 2017.
- [17] Yujia Li, Daniel Tarlow, Marc Brockschmidt, and Richard Zemel. Gated graph sequence neural networks. *arXiv preprint arXiv:1511.05493*, 2015.
- [18] Federico Monti, Davide Boscaini, Jonathan Masci, Emanuele Rodola, Jan Svoboda, and Michael M Bronstein. Geometric deep learning on graphs and manifolds using mixture model cnns. In *Proceedings of the IEEE Conference on Computer Vision and Pattern Recognition*, pages 5115–5124, 2017.
- [19] Bryan Perozzi, Rami Al-Rfou, and Steven Skiena. Deepwalk: Online learning of social representations. In *Proceedings of the 20th ACM SIGKDD international conference on Knowledge discovery and data mining*, pages 701–710. ACM, 2014.
- [20] Matthew E. Peters, Mark Neumann, Robert L Logan, Roy Schwartz, Vidur Joshi, Sameer Singh, and Noah A. Smith. Knowledge enhanced contextual word representations. In *EMNLP*, 2019.

- [21] Meng Qu, Jian Tang, Jingbo Shang, Xiang Ren, Ming Zhang, and Jiawei Han. An attention-based collaboration framework for multi-view network representation learning. In *Proceedings of the 2017 ACM on Conference on Information and Knowledge Management*, pages 1767–1776, 2017.
- [22] Franco Scarselli, Marco Gori, Ah Chung Tsoi, Markus Hagenbuchner, and Gabriele Monfardini. The graph neural network model. *IEEE Transactions on Neural Networks*, 20(1):61–80, 2008.
- [23] Prithviraj Sen, Galileo Namata, Mustafa Bilgic, Lise Getoor, Brian Galligher, and Tina Eliassi-Rad. Collective classification in network data. *AI magazine*, 29(3):93–93, 2008.
- [24] Nitish Srivastava, Geoffrey Hinton, Alex Krizhevsky, Ilya Sutskever, and Ruslan Salakhutdinov. Dropout: a simple way to prevent neural networks from overfitting. *The journal of machine learning research*, 15(1):1929–1958, 2014.
- [25] Lei Tang and Huan Liu. Uncovering cross-dimension group structures in multi-dimensional networks. In *SDM workshop on Analysis of Dynamic Networks*, pages 568–575. ACM, 2009.
- [26] Lei Tang, Xufei Wang, and Huan Liu. Uncovering groups via heterogeneous interaction analysis. In *2009 Ninth IEEE International Conference on Data Mining*, pages 503–512. IEEE, 2009.
- [27] Ashish Vaswani, Noam Shazeer, Niki Parmar, Jakob Uszkoreit, Llion Jones, Aidan N Gomez, Łukasz Kaiser, and Illia Polosukhin. Attention is all you need. In *Advances in neural information processing systems*, pages 5998–6008, 2017.
- [28] Petar Veličković, Guillem Cucurull, Arantxa Casanova, Adriana Romero, Pietro Lio, and Yoshua Bengio. Graph attention networks. *arXiv preprint arXiv:1710.10903*, 2017.
- [29] Xiang Wang, Dingxian Wang, Canran Xu, Xiangnan He, Yixin Cao, and Tat-Seng Chua. Explainable reasoning over knowledge graphs for recommendation. In *Proceedings of the AAAI Conference on Artificial Intelligence*, volume 33, pages 5329–5336, 2019.
- [30] Yang Ye and Shihao Ji. Sparse graph attention networks, 2019.
- [31] Hongming Zhang, Liwei Qiu, Lingling Yi, and Yangqiu Song. Scalable multiplex network embedding. In *IJCAI*, volume 18, pages 3082–3088, 2018.

A Supplementary Materials

A.1 Dataset Statistics

Table 4: Dataset Statistics

	Cora	Citeseer	PubMed	PPI	Twitter[†]	YouTube[†]
Node Classes	7	6	3	121	1	1
Edge Types	1	1	1	1	4	5
Node Features	1,433	3,703	500	50	0	0
Nodes	2,708	3,327	19,717	56,944	456,626	15,088
Edges	5,429	4,732	44,338	818,716	15,367,315	13,628,895
Training Nodes	140	120	60	44,906	9,990	2,000
Training Edges	—*	—*	—*	1,246,382	282,115	1,114,025
Validation Nodes	500	500	500	6,514	9,891	2,000
Validation Edges	—*	—*	—*	201,647	16,463	65,512
Testing Nodes	1,000	1,000	1,000	5,524	9,985	2,000
Testing Edges	—*	—*	—*	164,319	32,919	131,007
Neighbours per Node	3.9	2.7	4.4	28.3	28.2	557.0

[†] Shared nodes across dataset types with access to training set edges only.

* Access to all edges.

A.2 Experiment Settings

Table 5: Experiment Settings

Parameter	Node Classification		Link Prediction
	Transductive	Inductive	Transductive
Maximum number of steps (C)	3	3	2
Neighbourhood sample size (S)	10/100/500	10/100/500	100
Layer size (F, F', F'')	50	50	—
Node embedding size (R)	10	—	50
Edge type embedding size (D)	10	5	50
Number of attention heads	8	10	10
Input noise rate	0.9	0	0
Dropout probability	0.5	0	0
L_2 regularization coefficient (λ)	0.05	0	0
Learning rate	0.001	0.001	0.001
Maximum number of epochs	1000	1000	1000
Early stopping patience	100	10	5
Batch size (B)	5000	100	200